AGU PUBLICATIONS

Geophysical Research Letters

RESEARCH LETTER
10.1002/2016GL067671

Key Points:
- Downhole frictional strength is obtained using surface drilling torque
- Drilling torque data are acquired at seismic slip rates
- The frictional strength is comparable to that from friction experiments on recovered core samples

Supporting Information:
- Supporting Information S1

Correspondence to:
K. Ujiie,
kujiie@geol.tsukuba.ac.jp

Citation:
Ujiie, K., T. Inoue, and J. Ishiwata (2016), High-velocity frictional strength across the Tohoku-Oki megathrust determined from surface drilling torque, *Geophys. Res. Lett.*, *43*, 2488–2493, doi:10.1002/2016GL067671.

Received 5 JAN 2016
Accepted 24 FEB 2016
Accepted article online 1 MAR 2016
Published online 16 MAR 2016

High-velocity frictional strength across the Tohoku-Oki megathrust determined from surface drilling torque

Kohtaro Ujiie[1,2], Tomoya Inoue[3], and Junya Ishiwata[3]

[1]Graduate School of Life and Environmental Sciences, University of Tsukuba, Tsukuba, Japan, [2]Research and Development Center for Ocean Drilling Science, Japan Agency for Marine-Earth Science and Technology, Yokohama, Japan, [3]Center for Deep Earth Exploration, Japan Agency for Marine-Earth Science and Technology, Yokohama, Japan

Abstract High-velocity frictional strength is one of the primary factors controlling earthquake faulting. The Japan Trench Fast Drilling Project drilled through the shallow plate boundary fault, where displacement was ~50 m during the 2011 Tohoku-Oki earthquake. To determine downhole frictional strength, we analyzed the surface drilling torque data acquired at rotation rates equivalent to seismic slip rates (0.8–1.3 m/s). The results show a clear contrast in high-velocity frictional strength across the plate boundary fault: the apparent friction coefficient of frontal prism sediments (hemipelagic mudstones) in the hanging wall is 0.1–0.3, while that of the underthrust sediments (mudstone, laminar pelagic claystone, and chert) in the footwall increases to 0.2–0.4. The apparent friction coefficient of the smectite-rich pelagic clay in the plate boundary fault is 0.08–0.19, which is consistent with that determined from high-velocity (1.1–1.3 m/s) friction experiments. This suggests that surface drilling torque is useful in obtaining downhole frictional strength.

1. Introduction

Frictional strength at seismic slip rates is a key to evaluating fault weakening and rupture propagation during earthquakes. High-velocity friction experiments on fault zone materials and their analogs by rotary shear apparatuses have contributed greatly to the understanding of earthquake mechanics [*Di Toro et al.*, 2011, and reference therein]. Active fault zone drilling has also provided an invaluable opportunity to investigate earthquake dynamics [*Ma et al.*, 2006; *Tobin and Kinoshita*, 2006; *Chester et al.*, 2013a; *Li et al.*, 2013; *Ujiie and Kimura*, 2014]. The Integrated Ocean Drilling Program Expedition 343 and 343T, Japan Trench Fast Drilling Project (JFAST) drilled through the shallow portion of the plate boundary fault near the Japan Trench offshore of the Miyagi Prefecture, where huge displacements of ~50 m occurred during the 2011 Tohoku-Oki earthquake (M_w9.0) [*Chester et al.*, 2013a] (Figure 1). The coseismic frictional strength was estimated from the residual frictional heat associated with the Tohoku-Oki earthquake, which was detected by temperature measurements in the borehole [*Fulton et al.*, 2013]. The frictional strength of materials in the toe of the Japan Trench subduction zone was determined from friction experiments on recovered core samples [*Ujiie et al.*, 2013; *Ikari et al.*, 2015; *Remitti et al.*, 2015]. However, the frictional strength was obtained from only limited intervals at the drill site (Figure 1). This is because spot coring was conducted in short intervals during JFAST due to schedule delays associated with severe weather and technical difficulties of drilling at great water depths of ~6900 m. In 137 m of total coring intervals, the total length of recovered cores was only 53.31 m [*Chester et al.*, 2013a]. Thus, the downhole frictional strength in the large slip region of the Tohoku-Oki earthquake remains incomplete.

On the D/V *Chikyu*, surface drilling data were acquired during the drilling operations. These included drilling torque and weight on the drill bit measurements. In the JFAST study, the drilling torque represents the torque of the power swivel, which rotates the drill string. In this study, we used the drilling torque acquired at rotation rates equivalent to seismic slip rates to calculate the shear stress between the drill bit and geological formations. The weight on bit data was used for the estimation of the normal stress on the bit. On the basis of the calculated shear and normal stresses, we determined the downhole high-velocity frictional strength across the shallow plate boundary fault and compared it to the frictional strength obtained from high-velocity friction experiments on the plate boundary fault samples and from borehole temperature measurements.

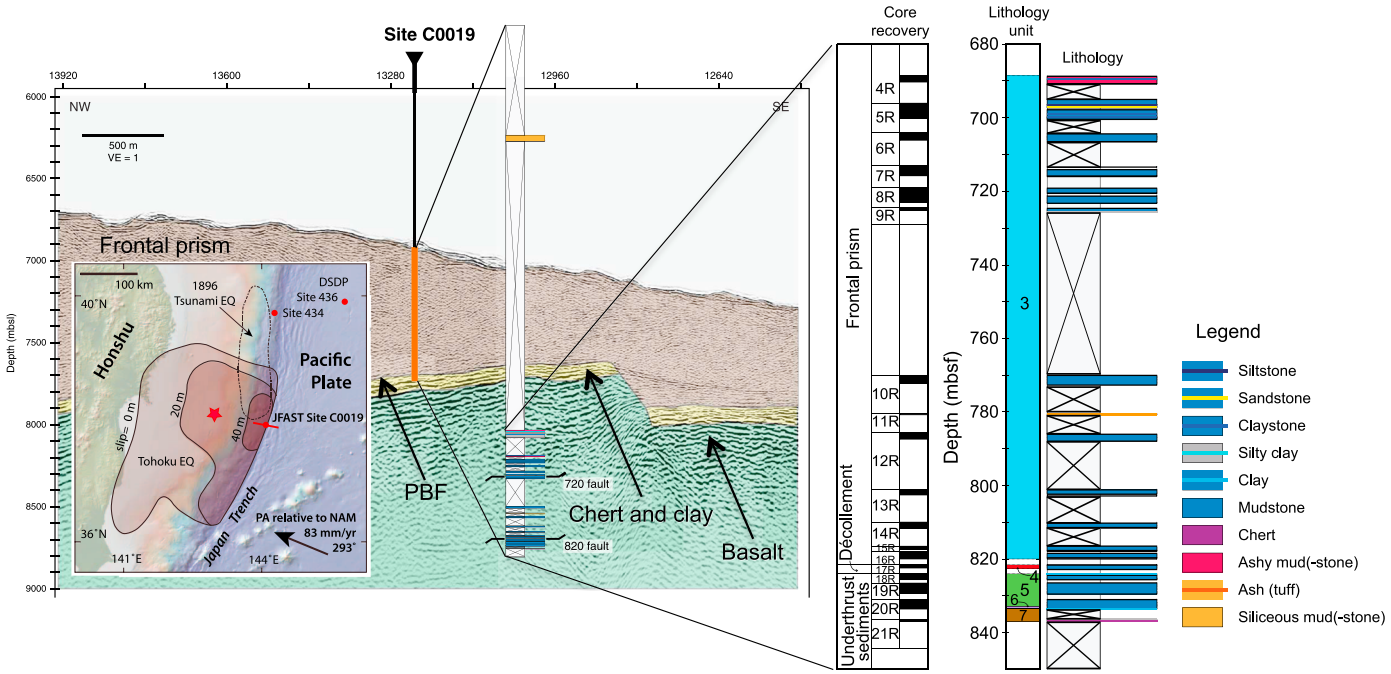

Figure 1. Seismic profile showing the location of the drill site C0019 in the toe region of the Japan Trench subduction zone. The frontal prism above the plate boundary fault (PBF) is characterized by acoustically chaotic seismic images, while chert and clay below the PBF are marked by subhorizontal reflectors. Core recovery, lithology unit, and lithology at 680–840 mbsf are shown at the right. Unit 3, hemipelagic mudstone; Unit 4, smectite-rich pelagic clay; Unit 5, brown mudstone; Unit 6, laminar pelagic claystone; and Unit 7, chert. The inset shows the coseismic slip distribution of the 2011 Tohoku-Oki earthquake [after *Chester et al.*, 2013b]. The red dots and star indicate ocean drilling sites and the epicenter of the Tohoku-Oki earthquake, respectively.

2. Methods

JFAST conducted logging while drilling, coring, and measuring temperature in different holes [*Chester et al.*, 2013a]. From these drill holes, we chose the coring hole for the estimation of downhole frictional strength. This enabled the direct comparison of frictional strength determined from different methods (i.e., surface drilling data versus laboratory experiments on recovered core samples) and also the determination of the effects of lithology on the frictional strength. We analyzed the surface drilling data at depths of 650–850 meters below seafloor (mbsf), which include the frontal prism and underthrust sediments above and below the plate boundary fault at ~820 mbsf, respectively [*Chester et al.*, 2013a, 2013b; *Kirkpatrick et al.*, 2015]. On the basis of observation and description of the recovered cores, the frontal prism consists of moderately to steeply dipping (~20–80°) olive-gray to very dark gray and grayish brown hemipelagic mudstones, while the underthrust sediments are composed of subhorizontal brown mudstone, laminar pelagic claystone, and chert (Figure 1). The plate boundary fault is dominated by the smectite-rich pelagic clay and is characterized by the development of scaly fabric associated with shearing [*Chester et al.*, 2013a, 2013b; *Ujiie et al.*, 2013; *Kameda et al.*, 2015; *Kirkpatrick et al.*, 2015]. The interval of scaly clay is 821.5 to 822.5 mbsf, but its upper and lower boundaries were not recovered in the cores. If the neighboring unrecovered portions are also composed of the scaly clay, the interval of the plate boundary fault will be 820.01–824 mbsf. This ~4 m thick interval is defined as the plate boundary fault zone.

To determine the slip rate during drilling, we adopted an equivalent slip rate V_e [*Shimamoto and Tsutsumi*, 1994] for the bottom surface of the drill bit by approximating the shape of the bottom surface to a hollow disk shape (Figures 2a and 2b):

$$V_e = \frac{\pi R\left(r_o^3 - r_i^3\right)}{45\left(r_o^2 - r_i^2\right)} \quad (1)$$

where R is the revolution rate of the drill bit, and r_i and r_o are the inner and outer radiuses of the hollow disk, respectively. We used the R values recorded during coring and used 2.9 cm and 13.4 cm for r_i and r_o, respectively. The calculated V_e ranges from 0.8 to 1.3 m/s. Thus, the drilling torque data were acquired at seismic slip rates.

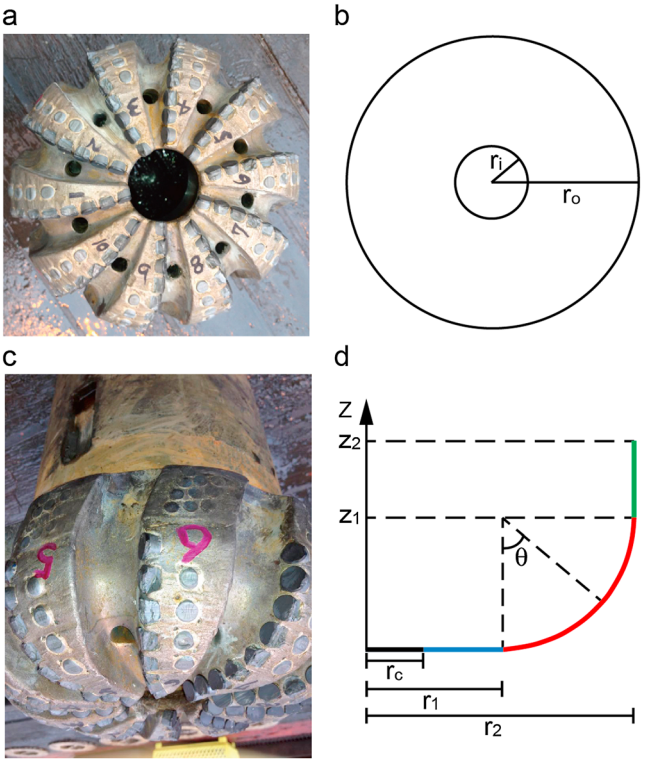

Figure 2. The configuration of the drill bit used for the coring during JFAST. (a) A photograph showing the bottom surface of the drill bit. (b) The shape of the bottom surface approximating to a hollow disk shape. (c) A photograph showing the three-dimensional shape of the drill bit. (d) The cross section of the drill bit composed of bottom (blue), circular arc (red), and side (green) surfaces.

The drill bit that was used at the coring site is a polycrystalline diamond cutter (PDC) bit (Figure 2). The PDC bit is designed considering a complicated drilling mechanism including cutting, friction, and the ejection process. The number of cutters, its angle, and the arrangement are determined in order to achieve efficient cutting performance. The torque exerted on the PDC bit is mainly decomposed into the torque during the cutting process and the torque associated with friction. The cutting torque is considerably affected by the design of the cutters, as well as unknown operational conditions such as actual facing angle (i.e., the angle of the drill bit facing to the drilling layer), torsional/lateral vibrations on the drill bit, and the weight on bit resulting in the depth of cut. Since it is difficult to accurately determine the cutting torque during operations due to the unknown conditions, there are some efforts being made to express the cutting torque practically, eventually leading to drilling torque. *Detounay and Defourny* [1992] assumed that the cutting torque is proportional to the depth of cut and concluded that frictional contact is a pervasive feature, and that the contact friction coefficient reflects the internal frictional property of the drilling layers. *Balanov et al.* [2003] assumed that the torque exerted on the drill bit is treated as a frictional torque based on the contacted area, which is a common assumption, for analyzing the bit motions such as stick slip and whirl. Thus, in this paper, we assume that the torque exerted on the PDC bit can be treated as the frictional torque, and the shear stress can be derived from the frictional torque and an active surface area of the vanes on the PDC bit.

The measured torque includes the viscous torque between the drill string and seawater, the frictional torque between the drill string and the borehole wall, and the frictional torque between the drill bit and the geological formations. To evaluate the first two, we used the torque data during bottom-up operations, which are given when the drill bit is hoisted up from the drilling layer with the power swivel rotating the drill string. We subtracted the torque during bottom-up operations from the measured torque during coring and obtained the frictional torque between the drill bit and geological formations (see supporting information). Then, we calculated the shear stress (τ) from the frictional torque (T), taking the configuration of the drill bit into consideration (Figure 2c). Assuming that τ is constant throughout the drill bit, and that T is the summation of the torques in the bottom, circular arc, and side surfaces (Figure 2d), T can be expressed as follows:

$$T = \frac{\tau}{2}\int_{r_c}^{r_1} 2\pi r^2 \mathrm{d}r + \frac{\tau}{2}\int_0^{\frac{\pi}{2}} 2\pi (r_1 + z_1 \sin\theta)^2 z_1 \mathrm{d}\theta + \frac{\tau}{2}\int_{z_1}^{z_2} 2\pi r_2^2 \mathrm{d}z \quad (2)$$

Equation (2) considers that τ does not appear in the channel parts of the drill bit, which occupy half of the bit volume.

The weight on bit was estimated from the hook load of the drill string (see supporting information). The normal stress (σ_n) during drilling was obtained by dividing the weight on bit by the projected contact area of the drill bit (~0.027 m^2), assuming that σ_n does not appear in the channel part of the drill bit. The apparent

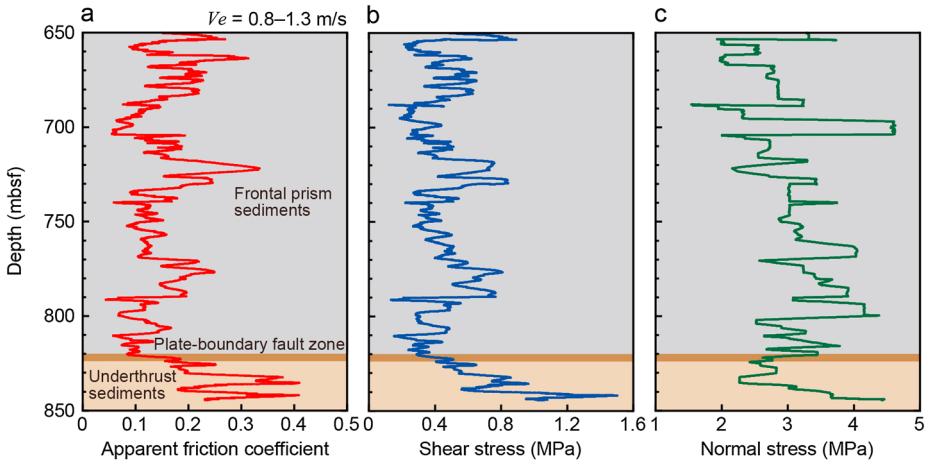

Figure 3. The downhole (a) apparent friction coefficient, (b) shear stress, and (c) normal stress determined from the surface drilling data.

friction coefficient (μ) is defined as τ/σ_n. To eliminate data spikes and oscillations, we averaged μ, τ, and σ_n data over 60 s and over 300 s and found that the latter is appropriate for evaluating downhole changes in μ, τ, and σ_n (see supporting information).

3. Results and Discussion

The downhole μ, τ, and σ_n obtained at depths of 650–850 mbsf are shown in Figure 3. The patterns of μ and τ are similar with depth, while σ_n fluctuates between 2 and 4 MPa. There are marked contrasts in μ and τ between the frontal prism sediments in the hanging wall and the underthrust sediments in the footwall. The μ values in the frontal prism sediments range from ~0.1 to 0.3, while those of the underthrust sediments increase to ~0.2–0.4. The μ values of the plate boundary fault zone range from 0.08 to 0.19 (Figure 4). The τ values in the frontal prism sediments range from ~0.2 to 0.8 MPa, while those of the underthrust sediments increase to ~0.4–1.5 MPa. The τ values of the plate boundary fault zone range from 0.29 to 0.51 MPa (Figure 4).

Since the surface drilling torque data during coring were acquired at rotation rates equivalent to seismic slip rates (0.8–1.3 m/s), the downhole μ data represent frictional strength at seismic slip rates. The μ values of ~0.1–0.3 in the frontal prism sediments are consistent with those of friction experiments on argillaceous materials at 1.3 m/s under wet (water-saturated) conditions [*Ujiie and Tsutsumi*, 2010; *Faulkner et al.*, 2011; *Bullock et al.*, 2015]. In these friction experiments, the steady state friction of ~0.1–0.3 was established almost immediately after the peak friction, showing a rapid slip weakening behavior with a negligible slip weakening distance. If unrecovered and uncored intervals in the frontal prism have similar lithologies to those in recovered cores, the μ values of ~0.1–0.3 could represent the friction coefficient of hemipelagic mudstones, which may vary with mineral composition such as clay content [*Ujiie et al.*, 2013; *Bullock et al.*, 2015]. Similarly, the μ

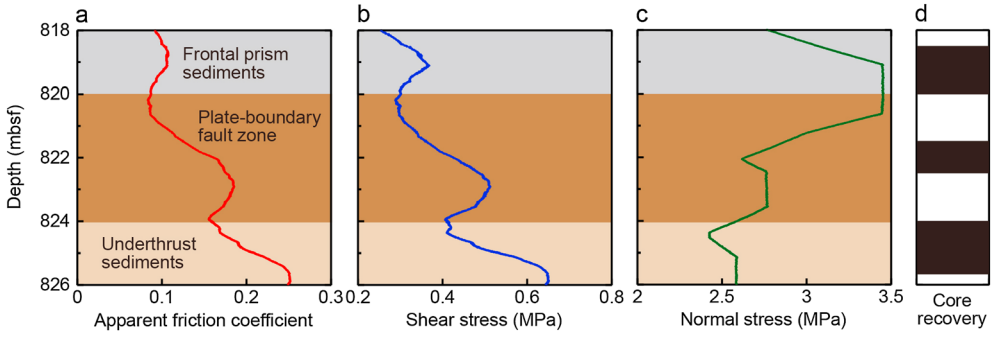

Figure 4. The close-up view of downhole (a) apparent friction coefficient, (b) shear stress, (c) normal stress, and (d) core recovery across the plate boundary fault zone.

values of ~0.2–0.3 in the underthrust sediments could also reflect the high-velocity frictional properties of brown mudstone. However, the μ values of ~0.3–0.4 in the underthrust sediments appear to be high when compared to the friction coefficient of argillaceous materials obtained at 1.3 m/s under wet conditions. The recovered cores in subducting material below the plate boundary fault include yellow-brown and chocolate-brown chert fragments [*Chester et al*., 2013a; *Kirkpatrick et al*., 2015], and the high-resolution seismic imaging in the toe region of the Japan Trench subduction zone suggests that chert layers were subducted beneath the frontal prism [*Nakamura et al*., 2013] (Figure 1). High-velocity (1.3 m/s) friction experiments on novaculite (chert composed of ~100% microcrystalline quartz) show a steady state friction of ~0.4 [*Di Toro et al*., 2006]. Therefore, it is likely that the increased μ values of ~0.3–0.4 in the underthrust materials represent the high-velocity frictional strength of chert.

High-velocity (1.1–1.3 m/s) friction experiments on the smectite-rich (60–80 wt%) pelagic clay from the plate boundary fault zone under wet and impermeable conditions showed a rapid slip weakening behavior with a steady state friction of 0.07–0.11 [*Ujiie et al*., 2013; *Remitti et al*., 2015]. However, in wet and permeable conditions, the value of the steady state friction after a rapid slip weakening was increased to 0.23 [*Ujiie et al*., 2013]. These friction experiments were conducted at normal stresses of 2.0–3.5 MPa, which were comparable to σ_n values during drilling at the plate boundary fault zone (~2.6–3.5 MPa) (Figure 4c). The μ values of the plate boundary fault zone determined from the surface drilling data are 0.08–0.19 (Figure 4a). The smaller μ values are consistent with those from the high-velocity friction experiments under wet and impermeable conditions [*Ujiie et al*., 2013; *Remitti et al*., 2015] and, therefore, likely represent the frictional strength of the smectite-rich pelagic clay at seismic slip rates under wet and impermeable conditions. The smaller μ values are also compatible with the apparent friction coefficient of 0.08 determined from the residual frictional heat from the Tohoku-Oki earthquake [*Fulton et al*., 2013]. On the other hand, the larger μ values may represent the high-velocity frictional strength of the smectite-rich pelagic clay under conditions that are between permeable and impermeable. Another possibility is that the larger μ values are in places derived from the frictional strength of brown mudstone in which weak clay (smectite) content is decreased to 20–40 wt% [*Kameda et al*., 2015]. The brown mudstone was found in the recovered core immediately below the plate boundary fault at ~824 mbsf [*Chester et al*., 2013a, 2013b; *Kirkpatrick et al*., 2015]. It is possible that brown mudstone is also present in the unrecovered interval. The 60 cm thick laminar pelagic claystone at ~833 mbsf in underthrust sediments shows variable smectite content of ~5 to ~60 wt %, with its highest values being comparable to that of the pelagic clay in the plate boundary fault zone [*Kameda et al*., 2015]. However, μ shows higher values of ~0.36. This may reflect the siliceous mineralization and the presence of siliceous microfossils in the laminar pelagic claystone, which are absent from the pelagic clay in the plate boundary fault zone [*Chester et al*., 2013a]. In addition, the interval of high smectite content (~60 wt %) in the laminar pelagic claystone is very narrow ($<$60 cm) and thus could be difficult to express in μ data that averaged over 300 s.

The drill bit tended to wear during drilling, possibly leading to a change in the surface area of the drill bit. This might affect the estimation of τ and σ_n from the surface drilling data. If a different type of the drill bit with more complicated configurations is used, the estimation of τ from the surface drilling torque will be difficult. The σ_n during coring was determined from the weight on bit that was estimated from the change in the hook load of the drill string. It is best to determine the weight on bit from the drill bit load sensor installed immediately above the drill bit rather than from the hook load of the drill string. Despite these difficulties, the results suggest that the downhole high-velocity frictional strength determined from the surface drilling data appears to show reasonable values, which are consistent with the frictional strength obtained from the friction experiments at seismic slip rates. Since core recovery in a fault zone is generally poor, and the coring intervals are sometimes restricted due to various operational reasons, the surface drilling data are invaluable in acquiring the continuous changes in frictional strength with depth. In these situations, the friction experiments on recovered core samples can be used to verify the friction data determined from the surface drilling data.

4. Conclusions

We analyzed the surface drilling data at the JFAST coring site and obtained the downhole high-velocity (0.8–1.3 m/s) frictional strength in the region of ~50 m slip during the Tohoku-Oki earthquake. The results indicate that the frictional strength at seismic slip rates is markedly different between the frontal prism

and underthrust sediments above and below the plate boundary fault, respectively. The μ of ~0.1–0.3 in the frontal prism sediments could represent the high-velocity frictional strength of the hemipelagic mudstones, while the increased μ of ~0.3–0.4 in the underthrust sediments is likely attributed to the presence of chert. The μ of 0.08–0.19 in the plate boundary fault zone is consistent with that determined from high-velocity (1.1–1.3 m/s) friction experiments on the smectite-rich pelagic clay recovered from the plate boundary fault zone. We conclude that surface drilling torque is useful in obtaining the profile of coseismic fault strength.

Acknowledgments
The drilling data are available from Center for Deep Earth Exploration, Japan Agency for Marine-Earth Science and Technology upon request. We thank the drilling operation staff on board the D/V *Chikyu* during JFAST. We are grateful for the thoughtful and helpful comments by Matt J. Ikari, two anonymous reviewers, and the Editor, Andrew Newman. K.U. is supported by Grant-in-Aid for Scientific Research (B) from JSPS (26287124).

References

Balanov, A., N. B. Janson, P. V. E. McClintock, R. W. Tucker, and C. H. T. Wang (2003), Bifurcation analysis of a neutral delay differential equation modeling the torsional motion of a driven drill string, *Chaos, Solitons Fractals*, *15*(2), 381–394.

Bullock, R. J., N. De Paola, and R. E. Holdsworth (2015), An experimental investigation into the role of phyllosilicate content on earthquake propagation during seismic slip in carbonate faults, *J. Geophys. Res. Solid Earth*, *120*, 3187–3207, doi:10.1002/2015JB011914.

Chester, F. M., J. Mori, N. Eguchi, S. Toczko, and the Expedition 343/343T Scientists (2013a), Japan Trench Fast Earthquake Drilling Project (JFAST), in *Proceedings of the IODP*, vol. 343/343T, Integrated Ocean Drill. Program Manage. Int., Inc., College Station, Tex., doi:10.2204/iodp.proc.343343T.2013.

Chester, F. M., et al. (2013b), Structure and composition of the plate-boundary slip-zone for the 2011 Tohoku-Oki earthquake, *Science*, *342*(6163), 1208–1211, doi:10.1126/science.1243719.

Detounay, E., and P. Defourny (1992), A phenomenological model for the drilling action of drag bits, *Int. J. Rock Mech. Min. Sci. Geomech. Abstr.*, *29*, 13–23.

Di Toro, G., T. Hirose, S. Nielsen, and T. Shimamoto (2006), Relating high-velocity rock-friction experiments to coseismic slip in the presence of melts, in *Radiated Energy and the Physics of Earthquake Faulting*, *Geophys. Monogr. Ser.*, vol. 170, edited by R. Abercrombie et al., pp. 121–134, AGU, Washington, D. C.

Di Toro, G., R. Han, T. Hirose, N. De Paola, S. Nielsen, K. Mizoguchi, F. Ferri, M. Cocco, and T. Shimamoto (2011), Fault lubrication during earthquakes, *Nature*, *471*(7339), 494–498, doi:10.1038/nature09838.

Faulkner, D. R., T. M. Mitchell, J. Behnsen, T. Hirose, and T. Shimamoto (2011), Stuck in the mud? Earthquake nucleation and propagation through accretionary forearcs, *Geophys. Res. Lett.*, *38*, L18303, doi:10.1029/2011GL048552.

Fulton, P. M., et al. (2013), Low coseismic friction on the Tohoku-Oki fault determined from temperature measurements, *Science*, *342*(6163), 1214–1217, doi:10.1126/Science.1243641.

Ikari, M. J., J. Kameda, D. M. Saffer, and A. J. Kopf (2015), Strength characteristics of Japan Trench borehole samples in the high-slip region of the 2011 Tohoku-Oki earthquake, *Earth Planet. Sci. Lett.*, *412*, 35–41, doi:10.1016/j.epsl.2014.12.014.

Kameda, J., M. Shimizu, K. Ujiie, T. Hirose, M. Ikari, J. Mori, K. Oohashi, and G. Kimura (2015), Pelagic smectite as an important factor in tsunamigenic slip along the Japan Trench, *Geology*, *43*, 155–158, doi:10.1130/G35948.1.

Kirkpatrick, J. D., et al. (2015), Structure and lithology of the Japan Trench subduction plate boundary fault, *Tectonics*, *34*, 53–69, doi:10.1002/2014TC003695.

Li, H., et al. (2013), Characteristics of the fault-related rocks, fault zones and the principal slip zone in the Wenchuan earthquake Fault Scientific Drilling Hole-1 (WFSD-1), *Tectonophysics*, *584*, 23–42, doi:10.1016/j.tecto.2012.08.021.

Ma, K.-F., et al. (2006), Slip zone and energetics of a large earthquake from the Taiwan Chelungpu-Fault Drilling Project, *Nature*, *444*, 473–476, doi:10.1038/nature05253.

Nakamura, Y., S. Kodaira, S. Miura, C. Regalla, and N. Takahashi (2013), High-resolution seismic imaging in the Japan Trench axis area off Miyagi, northeastern Japan, *Geophys. Res. Lett.*, *40*, 1713–1718, doi:10.1002/grl.50364.

Remitti, F., S. A. F. Smith, S. Mittempergher, A. F. Gualtieri, and G. Di Toro (2015), Frictional properties of fault zone gouges from the J-FAST drilling project (M_w 9.0 2011 Tohoku-Oki earthquake), *Geophys. Res. Lett.*, *42*, 2691–2699, doi:10.1002/2015GL063507.

Shimamoto, T., and A. Tsutsumi (1994), A new rotary-shear high-velocity frictional testing machine: Its basic design and scope of research (in Japanese with English abstract), *Struct. Geol.*, *39*, 65–78.

Tobin, H. J., and M. Kinoshita (2006), NanTroSEIZE: The IODP Nankai Trough Seismogenic Zone Experiment, *Sci. Drill.*, *2*, 23–27, doi:10.2204/iodp.sd.2.06.2006.

Ujiie, K., and G. Kimura (2014), Earthquake faulting in subduction zones: Insights from fault rocks in accretionary prisms, *Prog. Earth Planet. Sci.*, *1*, 1–30, doi:10.1186/2197-4284-1-7.

Ujiie, K., and A. Tsutsumi (2010), High-velocity frictional properties of clay-rich fault gouge in a megasplay fault zone, Nankai subduction zone, *Geophys. Res. Lett.*, *37*, L24310, doi:10.1029/2010GL046002.

Ujiie, K., et al. (2013), Low coseismic shear stress on the Tohoku-Oki megathrust determined from laboratory experiments, *Science*, *342*(6163), 1211–1214, doi:10.1126/science.1243485.